Outwards transport of angular momentum in a shallow water accretion disk experiment

F. Günzkofer[1,2] and P. Manz[3,2,1]
[1] *Physik-Department E28, Technische Universität München, James-Franck-Str. 1, 85748 Garching, Germany*
[2] *Max-Planck-Institut für Plasmaphysik, Boltzmannstr.2 ,85748 Garching, Germany*
[3] *Institute of Physics, University of Greifswald, 17489 Greifswald, Germany*
(Dated: April 28, 2021)

Accretion disks are an ubiquitous phenomenon in astrophysics. To be consistent with observations, there must be an as yet unknown mechanism for angular momentum redistribution. In laboratory experiments, especially the two dimensional geometry and the magnetohydrodynamic characteristics of an accretion disk are difficult to reproduce. Here we propose the design of a shallow water experiment in accretion disk geometry, where differential rotation is induced to a quasi-two dimensional shallow water layer with an open surface that allows direct measurement of the radial and azimuthal fluid dynamics. The effect of the magnetic field is mimicked by established equivalence of MHD and viscoelastic fluids. We demonstrate radial outward transport of angular momentum for the first time in an accretion disk laboratory experiment. Thereby, the proposed experimental setup can help to identify the origin of angular momentum redistribution in accretion disks.

PACS numbers:

I. INTRODUCTION

Accretion disks are one of the most common astrophysical phenomenons. Since the disk particles rotate on stable Keplerian orbits (with an angular velocity $\Omega \propto r^{-3/2}$ and radius r), the gas cannot accrete directly onto the central object without first losing angular momentum. How angular momentum is transported outwards to spin up the outer parts of the accretions disk and decelerate the inner parts to spiral onto the central object is one of the central questions. As molecular viscosity in accretion disks is small, an anomalous viscosity is needed to transport the angular momentum outwards. Turbulence can provide such anomalous viscosity. A possible instability leading to outward momentum transport is the magneto-rotational instability (MRI) [1] driven by weak magnetic fields. Due to the high conductivity of the accretion disk plasma, magnetic field lines are frozen-in and connect particles at different orbit radii similar to springs. The sheared rotation then leads to angular momentum transport from the inner to the outer particle.

There have been substantial efforts to demonstrate the MRI in laboratory experiments using different approaches to obtain sheared rotation of an MHD fluid. Experiments using a liquid Gallium alloy have been conducted in Taylor-Couette geometry and various magnetic field geometries [3–5]. Evidence for the magneto-rotational instability in such experiments has been found investigating fluctuations of the coaxial fluid flow [4, 5]. Other approaches included the use of liquid sodium in differential rotating spheres [6] and experiments with plasmas [7, 8] in Taylor-Couette geometry. Though Ref. [6] reported signs of the MRI, it should be mentioned that numerical simulations suggested these to be rather caused by different instabilities [9, 10]. Therefore any experimental findings on the MRI have to be carefully assessed in the light of other possible instabilities. To the best of our knowledge, enhanced outwards transport of angular momentum has not been demonstrated so far in any Taylor-Couette laboratory experiment.

We wonder if perhaps another geometry might be better suited to study the MRI. The experimental setup of the shallow water analogue of the standing accretion shock instability (SWASI) [11] seems to represent the geometry of the accretion disk more naturally. The setup would additionally have the practical advantage of an open fluid surface allowing for measurements of radial-azimuthal fluid dynamics which are necessary to estimate radial angular momentum transport. However, the shallow depth of the experiment is a concern since enhanced viscous damping is to be expected compared to the Taylor-Couette geometry. Furthermore, we were not sure whether angular momentum can be introduced into the system at all. We decided to give it a try.
The paper is organized as follows: In Sec. 2 the experimental setup is introduced. Angular rotation profiles are measured in water (Sec. 3) and compared to a viscoelastic fluid mimicking MHD effects (Sec. 4).

II. EXPERIMENTAL SET-UP

We propose an experiment of similar geometry as the one used to study the standing accretion shock instability [11]. A schematic depiction is shown in Fig. 1. Similar to Taylor-Couette geometry experiments, it exhibits an inner and outer radius of $r_{in} = 26$ mm and $r_{out} = 250$ mm, respectively. However, the upper boundary is a free surface and the lower boundary has a reciprocal shape

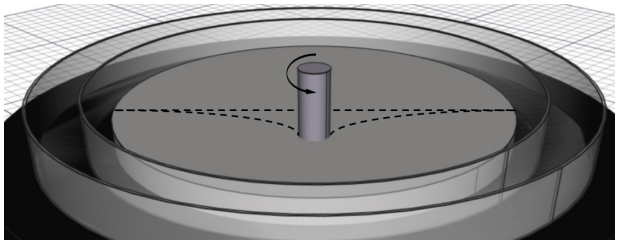

FIG. 1: Computer-aided design schematic of a reciprocal shaped fluid pool experiment to replicate an accretion disk geometry.

$$H(r) = -\frac{1000\ \mathrm{mm}^2}{r} + 4\ \mathrm{mm}. \tag{1}$$

leading to a very small aspect ratio $H/\left(r_{out} - r_{in}\right) \ll 1$ resembling accretion disk geometry. In standing accretion shock experiments, this lower boundary profile mimics a gravitational potential due to the shallow water approximation [11, 12].

Details on the experimental setup used here can be found in Ref. [12]. Different to the standing accretion shock instability experiment [12], the central cylinder is placed above the filling level, so no radial flow is forced externally. External momentum input is provided by rotation of the central drain. Rotation of the inner cylinder is obtained by attachment of a stepper motor and angular momentum is thereby induced into the fluid. Due to the shallow water analogy, a constant height h above the ground profile (see Eq. 1) favors Keplerian rotation. However, the pool is completely filled with fluid and thus in this experimental set-up does not yield Keplerian rotation since the lower boundary does not affect the surface rotation. This set-up resembles a Taylor-Couette-similar experiment with stationary outer cylinder. Compared to a flat bottom boundary, the reciprocal ground profile in Eq. 1 significantly enlarges the ratio of drain to bottom boundary and thereby allows for a better momentum induction to the fluid at a low thickness to radius ratio of the fluid disk. Though not necessarily Keplerian, a differential rotation is obtained nevertheless and the quasi-two dimensional geometry of an accretion disk is replicated. Additionally, the open surface allows in-situ measurements of the radial and azimuthal flow and thereby a direct detection of angular momentum transport. The height of the fluid h does not imitate the actual height of the accretion disk, which increases with the radius.

The MHD character of the accretion disk matter is central to the MRI mechanism. While both Reynolds and Maxwell stress contribute to outward transport of angular momentum, theoretical analysis has shown that this transport is dominated by the Maxwell stress for rotation profiles $\Omega(r)$ expected in accretion disks [13]. Plasma matter or liquid metals rotating in an external magnetic field are important for replication of an accretion disk system. However, such experiments require a rather expensive experimental set-up. Magnetic field lines acting as elastic springs within an MHD fluid can be replicated using a viscoelastic solution of long-chain polymers in water [14, 15]. The resulting polymeric stress tensor is similar to the magnetic stress tensor in MHD equations. Analytical and numerical investigations have shown the existence of an MRI-type instability for rotating viscoelastic fluids in Taylor-Couette geometry [15, 16]. Experiments found an instability analog to the MRI by analysing the coaxial mode numbers [17]. In the presented experimental prototype, experiments have been carried out with a viscoelastic solution to mimic MHD effects due to cost constraints. For comparison, experiments using only water to switch off any effects from MHD/viscoelastics have been performed.

The flow fields at the fluid surface are determined by Particle Tracking Velocimetry based on the Crocker-Grier algorithm [18]. Small tracer particles (Polypropylene spheres, $d = 3$ mm, $\rho = 0.9$ g cm^{-3}) are placed on the surface and move with the fluid flow. By a camera mounted approximately 1.4 m above the pool, the particle motion can be tracked. The particle velocities at different locations on the surface can be calculated and thereby the fluid rotation at different positions of the surface can be determined.

III. ROTATION PROFILES IN WATER

Whether hydrodynamic instabilities contribute to angular momentum transport in accretion disks in a non-negligible amount is not finally determined yet [19]. Experimental evidence so far indicates the influence of hydrodynamic instabilities to be small [20]. We first describe the experiments performed in water. Fig. 2 shows the rotational frequency $\Omega(x, y)$ in water in the central parts of the pool.

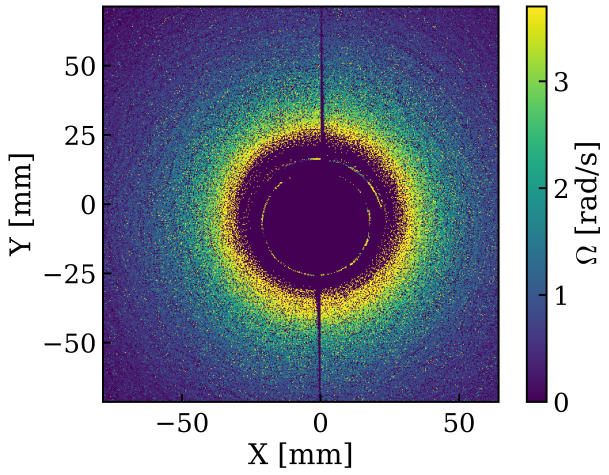

FIG. 2: Ω-map of water rotating in the pool as it is obtained by means of particle tracking velocimetry.

The azimuthal symmetry of the rotation shown in

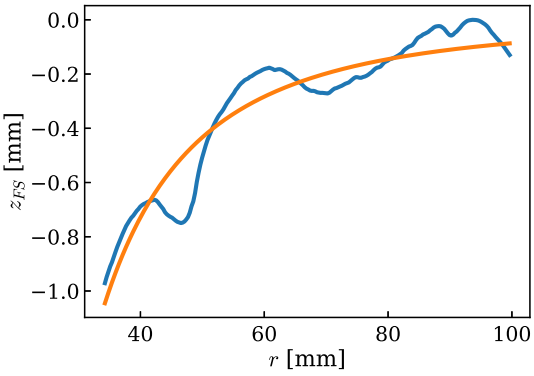

FIG. 3: Radial height profile (blue) shows that the measured $\Omega(r)$ results from an equilibrium of surface height gradient which can be obtained from the fit function (orange) and centrifugal force.

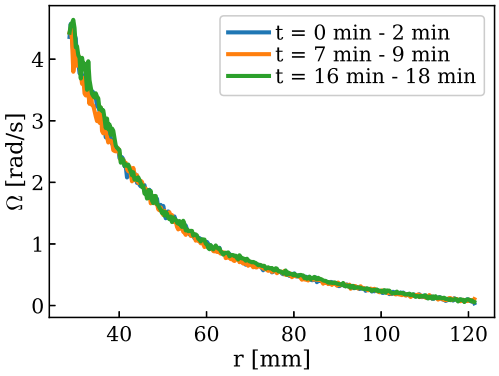

FIG. 4: Rotation profiles of purely hydrodynamic fluids are stable even for long rotation spans.

Fig. 2 allows for the calculation of the rotation profile. By means of Particle Tracking Velocimetry, a differential rotation profile $\Omega(r) \propto r^{-2.14}$ is found for water rotation in the region 26 mm $< r <$ 120 mm. The fitted exponent depends on the considered radial range and generally steepens if only outer regions are considered. However, $\mathrm{d}\ln\Omega/\mathrm{d}\ln r < -2$ holds for any choice of radial range. The capability of the Particle Tracking Velocimetry method can be tested by using the Fourier Transform Profilometry (FTP) established in previous experiments [12]. The FTP allows to measure height shifts at the free water surface z_{FS}. For stationary rotation, an equilibrium of the surface profile gradient and the centrifugal force due to rotation gives $\mathrm{d}z_{FS}/\mathrm{d}r = \Omega(r)^2 r$ which allows to compare rotation and height measurements. Fig. 3 shows the averaged surface height profile $z_{FS}(r) \propto r^{-2.33\pm0.06}$ which fits the expected $\mathrm{d}z_{FS}/\mathrm{d}r \propto r^{-3.28}$ quite well.

The radial decrease in angular frequency is much stronger than for the Keplerian case $\Omega(r) \propto r^{-3/2}$ in accretion disks. As mentioned above, the measured profile does not fulfill the requirements of a quasi-Keplerian profile since $\left|r^2\Omega\right|$ decreases with the radius as well. Such a rotation profile with $\mathrm{d}\ln\Omega/\mathrm{d}\ln r < -2$ is susceptible to Rayleigh's centrifugal instability. Presumably, the $\Omega \propto r^{-2.14}$ profile is the result of a balance between angular momentum transport by the Reynolds stress driven by the centrifugal instability and the bottom boundary drag damping the profile. Such a balance can lead to a stationary rotation profile.

Fig. 4 shows the rotation profiles $\Omega(r)$ averaged over consecutive time intervals. It can be seen that $\Omega(r) \propto r^{-2.14}$ remains constant for water even over longer time spans up to at least 18 minutes. The drain rotation is started at $t = 0$ and the data acquisition starts subsequently. Though it takes a few seconds for the water disk to spin up, this is not visible after averaging over a two minute interval. However, the kinematic viscosity ν of water and the observed area $A = \pi \cdot (120\ \mathrm{mm})^2$ allow to estimate the viscous momentum diffusion time $\tau = A/\nu \gg 18$ min. This already indicates that viscous momentum diffusion is negligible compared to other momentum transport processes.

The ground friction dampens the rotation profile towards $\Omega \to 0$. Since the ground friction acts as a momentum sink especially in the more shallow outer region of the pool, some process of outward angular momentum transport is required to maintain a stationary rotation profile $\Omega(r)$. The steep gradient of the rotation profile $\mathrm{d}\ln\Omega/\mathrm{d}\ln r < -2$ explicitly allows Rayleigh's centrifugal instability and therefore the obtained results can be explained without other hydrodynamic instabilities which might play a role for accretion disk dynamics. This is in good agreement with the results found in Ref. [20]. However, the presence of nonlinear instabilities, which are also discussed for accretion disks [19], additionally to the centrifugal instability can not be ruled out. Such instabilities are generally not expected to occur at the Reynolds numbers expected in the experiments presented here $Re \lesssim 4000$ [20].

IV. ROTATION PROFILES IN A VISCOELASTIC FLUID

The same measurements have been performed with the described viscoelastic polymer solution instead of water. The preparation of a viscoelastic fluid is based on the investigations done in Ref. [21]. A solution of Polyethylene glycol (PEG) and Polyethylene oxide (PEO) is used, where PEO - as a very-long-chain polymer - contributes the elastic properties of the fluid. For the measurements presented here, the used concentrations are $C_{PEG} = 15\%$ and $C_{PEO} = 1000$ ppm.

Fig. 5 shows a comparison of the rotation profiles for water and a viscoelastic fluid. Due to the process of rod

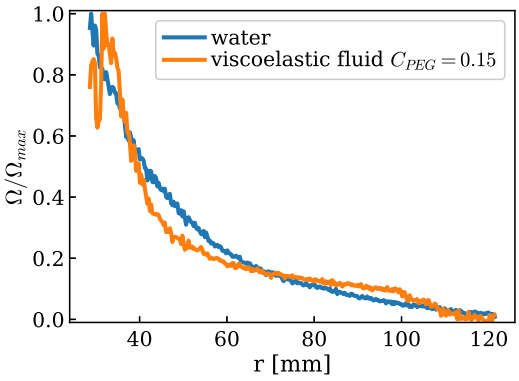

FIG. 5: Rotation profile comparison for water and a viscoelastic fluid (corresponding to $t = 120$ s–240 s after the drain rotation started in Fig. 7). Due to the higher momentum transfer from the central cylinder to the viscoelastic fluid compared to water, the rotation profiles are given in relative terms.

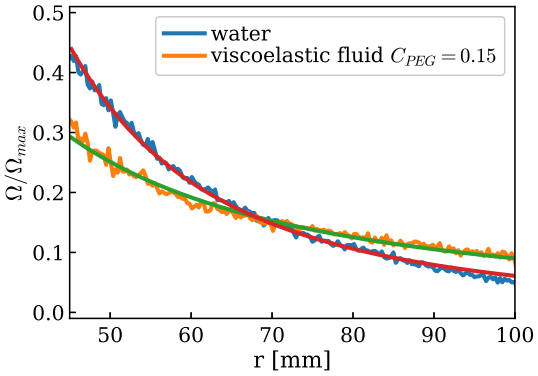

FIG. 6: Profile flattening region observed for a viscoelastic polymer solution (experimental data is shown in orange, fit in green) compared to water (experimental data is shown in blue, fit in red).

climbing caused by the Weissenberg effect [22], flow measurements close to the inner cylinder are not possible in a reliable way. At radii larger than 100 mm, fluid rotation is dominated by an increased influence of ground friction. The rotation is damped towards $\Omega \to 0$. Therefore, the region of interest of the shown measurements is restricted to radii 35 mm $< r <$ 100 mm.

The most prominent feature of the profile comparison is the region of profile flattening for 45 mm $\lesssim r \lesssim$ 100 mm as it is expected for enhanced outward transport of angular momentum. The accompanying region of profile steepening at 35 mm $\lesssim r \lesssim$ 45 mm fits the predictions of numerical analysis of the helical MRI in liquid metal experiments [23].

Fig. 6 shows the obtained relative rotation profiles Ω/Ω_{max} for viscoelastic and purely hydrodynamic fluid

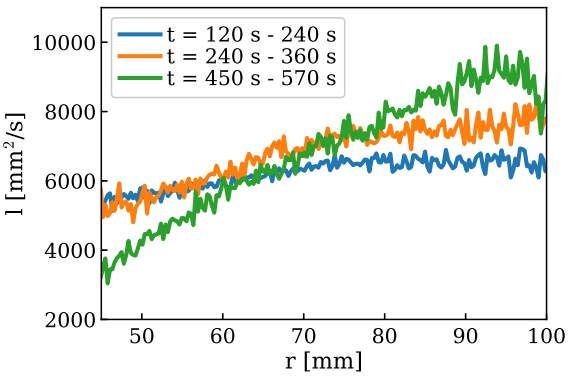

FIG. 7: The specific angular momentum l profile. For $r \gtrsim 100$ mm the specific angular momentum drops presumably due to the increased influence of ground friction.

rotation in the region of profile flattening. In the viscoelastic case, a fit of the angular velocity profile yields $\Omega(r) \propto r^{-1.56}$ which is very close to the ideal Keplerian profile of $\Omega(r) \propto r^{-3/2}$. Even though one might think that the flattening of the angular frequency profile can be attributed to the increased internal fluid friction (viscosity), the flow shear profile cannot be affected by the viscosity [21]. The ideal Taylor-Couette profile is only modified by advection of momentum due to a mean radial velocity, the Reynolds stress or the Maxwell stress or its viscoelastic equivalent respectively [24]. The boundary condition at the pulled up drain does not allow for a mean radial velocity. Fig. 4 showed that centrifugal instabilities, which are not possible for the profile in the flattening region, and the angular momentum transport due to the Reynolds stress are balanced by the bottom drag at a far steeper profile. The additional transport causing the profile to flatten can likely be attributed to an enhanced contribution of the viscoelastic Maxwell stress analogue.

The evolution of the specific angular momentum profile $l(r) = \Omega r^2$ profile over several minutes is shown in Fig. 7. Due to the mentioned rod climbing effect, the data acquisition is only started a sufficient time after the drain rotation when this process has reached an equilibrium so it does not influence the rotation profile.

Fig. 7 shows a transient event that lasts several minutes. Transient growth can occur due to the non-normality of the dynamical evolution operator. The MRI can be subject to nonmodal growth [25]. Due to the analogy of MHD to viscoelastic fluids, non-normal growth should be possible in the viscoelastic fluid as well. During this event, specific angular momentum is reduced for radii smaller than 60 mm and increased for radii larger than 60 mm. The specific angular momentum is transported radially outwards. It should be noted that all profiles shown in Fig. 7 fulfill the Rayleigh stability criterion $\mathrm{d}l/\mathrm{d}r > 0$. The observed momentum trans-

port can therefore not be explained by Rayleigh's centrifugal instability. The significantly larger viscosity of the viscoelastic solution compared to water ($\nu_{solution} \sim 10^2\ \nu_{water}$) results in a viscous diffusion time similar to the observed time of the transient event in Fig. 7. However, the increased specific angular momentum at the outer radii ($r > 70$ mm) seems not to be explainable with viscous diffusion. Viscous angular momentum diffusion is driven by a torque $M(r) = \iint r^2 t_{r\theta} \mathrm{d}\theta \mathrm{d}z$ arising from the viscous stress tensor component $t_{r\theta} \propto r\partial_r\Omega$. For $M(r) = const$, no net transport of angular momentum occurs. Neglecting the bottom drag, the viscosity damps the profile towards $\Omega(r) \to \Omega_0 r^{-2}$ corresponding to $l(r) = \text{const}$. At $t < 240$ s, $l(r)$ is closest to constant, the observed steepening of $l(r)$ at later times is not expected to be a result of enhanced viscosity. With increasing viscosity, also the bottom drag increases significantly. This is shown in Fig. 5, in the viscoelastic case $\Omega \to 0$ is found at large radii ($r > 100$ mm), where in water Ω remains finite. An increase of l, hence Ω as well, can also not be explained by enhanced bottom drag. Therefore, the observed profile steepening can not be explained by viscous momentum diffusion. This leaves the viscoelastic Maxwell stress as the most apparent cause for the observed transport during this transient event.

V. SUMMARY AND CONCLUSIONS

In summary, it is investigated if the shallow water approximation based accretion disk-like geometry proposed by Foglizzo et al. [11] is suitable to study the dynamics of accretion disks in laboratory experiments. The set-up geometry is closer to the accretion disk geometry than in Taylor-Couette experiments regarding the aspect ratio of radial and coaxial extension. When operating with liquid metals, the shallow water approximation may allow to investigate a rather large surface area at small fluid volume. Due to cost reasons, the here presented experiment prototype has been performed with a viscoelastic fluid instead of a liquid metal. Angular momentum transport is of main interest in the dynamics of accretion disks. In the present work, the rotation profiles have been measured by means of Particle Tracking Velocimetry. The experiments have been performed in water (purely hydrodynamic case) and in a solution of Polyethylene glycol and Polyethylene oxide (viscoelastic fluid). The comparison of these measurements allows to investigate the importance of magneto-hydrodynamic (MHD) effects for angular momentum transport. The experiments performed in the viscoelastic fluid showed a close to Keplerian rotation profile relevant for accretion disk dynamics.

The rotation measurements presented here support the idea of magnetohydrodynamical mechanisms being the likely cause of enhanced outwards transport of angular momentum in accretion disks. This indirectly also supports the magneto-rotational instability. While the rotation profiles of water appeared stable over time, the specific angular momentum reduces at small radii and increases at large radii in a viscoelastic fluid. This can be seen as enhanced angular momentum transport from small to large radii. An unambiguous identification of the driving instability in the present experiment has not been possible so far. However, the here presented prototype experiment shows a first promising result (i.e. outward angular momentum transport), hopefully motivating more detailed studies in this geometry in the future.

For accretion disks it is expected that both Reynolds and Maxwell stress lead to outward transport of angular momentum [13]. In future work, the different contributions of the Reynolds stress and the viscoelastic analogue of the Maxwell stress should be estimated. Direct measurements of radial and azimuthal velocities for example with Laser Doppler Velocimetry would allow for measurements of the Reynolds stress. Hereby, the refractive index transition at the open fluid surface is used to determine the surface flow velocities in radial and azimuthal direction from the Doppler shift in the reflected light. Measurement of radial fluid flows would also allow to investigate the impact of Ekman circulation effects. Additional measurements of the axial dynamics would be beneficial. Due to the large contact area at the pool bottom, Ekman effects are presumably highly influential in the presented set-up geometry [26]. However, whether these effects have a significantly higher impact in a viscoelastic fluid compared to water is not apparent and requires further investigation.

Acknowledgements

We thank Ulrich Stroth for his continuous support. Technical support by the E2M workshop, in particular Arne Friedrich and Robert Gieb, is gratefully acknowledged. P.M. acknowledges the stimulating environment of the 'Zugspitze meeting on turbulence', which was organized by Eberhard Bodenschatz (MPI for Dynamics and Self-Organization, Göttingen).

[1] S. A. Balbus and J. F. Hawley, Instability, turbulence, and enhanced transport in accretion disks, *Rev. Mod. Phys.* **70**, 1 (1998).

[2] S. A. Balbus, Enhanced Angular Momentum Transport in Accretion Disks, *Annual Review of Astronomy and Astrophysics* **41**, 555 (2003).

[3] R. Hollerbach and G. Rüdiger, New Type of Magnetorotational Instability in Cylindrical Taylor-Couette Flow, *Phys. Rev. Lett.* **95**, 124501 (2005).

[4] F. Stefani, T. Gundrum, G. Gerbeth, G. Rüdiger, M. Schultz, J. Szklarski, and R. Hollerbach, Experimental Evidence for Magnetorotational Instability in a Taylor-

Couette Flow under the Influence of a Helical Magnetic Field *Phys. Rev. Lett.* **97**, 184502 (2006).

[5] M. Seilmayer, V. Galindo, G. Gerbeth, T. Gundrum, F. Stefani, M. Gellert, G. Rüdiger, M. Schultz, and R. Hollerbach, Experimental Evidence for Nonaxisymmetric Magnetorotational Instability in a Rotating Liquid Metal Exposed to an Azimuthal Magnetic Field, *Phys. Rev. Lett.* **113**, 024505 (2014).

[6] D. R. Sisan, N. Mujica, W. A. Tillotson, Y.-M. Huang, W. Dorland, A. B. Hassam, T. M. Antonsen, and D. P. Lathrop, Experimental Observation and Characterization of the Magnetorotational Instability, *Phys. Rev. Lett.* **93**, 114502 (2004).

[7] C. Collins, N. Katz, J. Wallace, J. Jara-Almonte, I. Reese, E. Zweibel, and C. B. Forest, Stirring Unmagnetized Plasma, *Phys. Rev. Lett.* **108**, 115001 (2012).

[8] K. Flanagan, M. Clark, C. Collins, C. M. Cooper, I. V. Khalzov, J. Wallace, and C. B. Forest, Prospects for observing the magnetorotational instability in the plasma Couette experiment, *Journal of Plasma Physics* **81**, 345810401 (2015).

[9] R. Hollerbach, Non-axisymmetric instabilities in magnetic spherical Couette flow, *Proceedings of the Royal Society A: Mathematical, Physical and Engineering Sciences* **465**, 2003–2013 (2009).

[10] C. Gissinger, H. Ji, and J. Goodman, Instabilities in magnetized spherical Couette flow, *Phys. Rev. E* **84**, 026308 (2011).

[11] T. Foglizzo, F. Masset, J. Guilet, and G. Durand, Shallow Water Analogue of the Standing Accretion Shock Instability: Experimental Demonstration and a Two-Dimensional Model, *Phys. Rev. Lett.* **108**, 051103 (2012).

[12] S. Sebold, F. Günzkofer, R. Arredondo, T. Höschen, U. von Toussaint, U. Stroth, P. Manz, Advective-acoustic cycle in a shallow water standing accretion shock experiment, *Phys. Rev. E* **102**, 063103, (2020).

[13] M. E. Pessah, C. Chan and D. Psaltis, The signature of the magnetorotational instability in the Reynolds and Maxwell stress tensors in accretion discs, *Monthly Notices of the Royal Astronomical Society* **372**, 183-190, (2006).

[14] G. I. Ogilvie, M. R. E. Proctor, On the relation between viscoelastic and magnetohydrodynamic flows and their instabilities, *Journal of Fluid Mechanics* **476**, 389, (2003).

[15] G. I. Ogilvie, A.T. Potter, Magnetorotational-type instability in Couette-Taylor flow of a viscoelastic polymer liquid, *Phys. Rev. Lett.* **100**, 074503, (2008)

[16] Y. Bai, O. Crumeyrolle, and I. Mutabazi, Viscoelastic Taylor-Couette instability as analog of the magnetorotational instability *Phys. Rev. E*, **92**, 031001 (2015).

[17] S. Boldyrev, D. Huynh, V. Pariev, Analog of astrophysical magnetorotational instability in a Couette-Taylor flow of polymer fluids, *Phys. Rev. E* **80**, 066310, (2009)

[18] J. C. Crocker, D. G. Grier, Methods of digital video microscopy for colloidal studies, *Journal of colloid and interface science, Elsevier* **179**, 298-310, (1996).

[19] S. Fromang, G. Lesur, Angular momentum transport in accretion disks: a hydrodynamical perspective, *EAS Publications Series, EDP Sciences* **82**, 391-413, (2019).

[20] H. Ji, M. Burin, E. Schartman, J. Goodman, Hydrodynamic turbulence cannot transport angular momentum effectively in astrophysical disks, *Nature* **444**, 343–346, (2006).

[21] Y. Bai, Study of viscoelastic instabily in Taylor-Couette system as an analog of the magnetorotational instability (https://tel.archives-ouvertes.fr/tel-01255319, PhD thesis, Universite du Havre, France, 2015).

[22] K. Weissenberg, A continuum theory of rhelogical phenomena, *Nature* **159**, 310–311 (1947).

[23] G. Mamatsashvili, F. Stefani, A. Guseva and M. Avila, Quasi-two-dimensional nonlinear evolution of helical magnetorotational instability in a magnetized Taylor–Couette flow, *New Journal of Physics* **20**, 013012, (2018).

[24] E. Schartman, H. Ji, M. Burin, J. Goodman, Stability of quasi-Keplerian shear flow in a laboratory experiment, *Astronomy & Astrophysics* **543**, A94, (2012).

[25] J. Squire and A. Bhattacharjee, Nonmodal Growth of the Magnetorotational Instability, *Phys. Rev. Lett.* **113**, 025006, (2014).

[26] M.J. Burin, H. Ji, E. Schartman, R. Cutler, P. Heitzenroeder, W. Liu, L. Morris and S. Raftopolous *Experiments in Fluids* **40**, 962–966, (2006).